Heterogeneous Photodegradation of Pentachlorophenol and Iron Cycling with Goethite, Hematite and Oxalate under UVA Illumination

Qing Lan [a, b, d], Fang-bai Li [b, *], Cui-xiang Sun [b], Cheng-shuai Liu [b], Xiang-zhong Li [c]

[a] *Guangzhou Institute of Geochemistry, Chinese Academy of Sciences, Guangzhou 510640, PR China*

[b] *Guangdong Key Laboratory of Agricultural Environment Pollution Integrated Control, Guangdong Institute of Eco-Environmental and Soil Sciences, Guangzhou 510650, PR China*

[c] *Department of Civil and Structural Engineering, The Hong Kong Polytechnic University, Hong Kong, PR China*

[d] *Graduate University of Chinese Academy of Sciences, Beijing 100039, PR China*

Abstract

Heterogeneous photodegradation of pentachlorophenol (PCP) in the goethite (α-FeOOH) and hematite (α-Fe_2O_3) systems with oxalate under UVA illumination was investigated. The PCP degradation, dechlorination and detoxification, in terms of Microtox acute toxicity, were achieved to the higher efficiency in the hematite suspension than in the goethite suspension. The optimal initial concentration of oxalic acid (C^0_{ox}) for the PCP degradation with goethite and hematite under the experimental conditions was found to be 1.2 mM, since sufficient Fe(III) as $Fe(C_2O_4)_3^{3-}$ and Fe(II) as $Fe(C_2O_4)_2^{2-}$ can be formed at $C^0_{ox}\geq$1.2 mM. The main intermediates of PCP degradation were identified through GC-MS, HPLC and IC analyses. It was found that the cycling process between Fe(III) and Fe(II) in both the goethite and hematite systems occurred more vigorously at the initial stage and gradually became gentle, while the rate of PCP photodegradationvaried from fast to slow during the reaction time. furthermore, the formation of H_2O_2 during photoreaction was also studied to explore its effects on the photodegradation and the iron cycling processes.

Keywords: Heterogeneous photodegradation; pentachlorophenol; iron cycle; goethite; hematite; oxalate

**Corresponding author phone: 86-20-87024721; fax: 86-20-87024123; e-mail: cefbli@soil.gd.cn and cefbli@hotmail.com (Dr. Fangbai Li).*

1. Introduction

Iron, as the fourth most abundant element of the earth's crust, is rich in the environment. Oxalic acid, mainly secreted by plant roots [1] or formed by incomplete combustion of hydrocarbons [2, 3], is ubiquitous in soil, water and atmosphere. In nature, iron, oxalic acid, and sunlight can establish a homogeneous photo-Fenton-like system where iron exists in a dissolved form or a heterogeneous photo-Fenton-like system where iron is in a solid form. The heterogeneous Fe(III)-oxalate system should be more applicable to the natural environment, because the iron species are mostly present as amorphous or (hydr)oxides. In the 1990s several research groups [4-8] studied the mechanismsof iron (hydr)oxides dissolution in aqueous oxalate solution. Sulzberger's group explored the degradation of diuron in a goethite-oxalate system irradiated by UV [9]. Our group studied the effects of reaction conditions and the distribution of various iron species in the iron oxide-oxalate-UV system [10-13]. It is generally accepted that the reaction mechanisms of such a heterogeneous system include several critical processes. The chemical adsorption of oxalic acid first occurs on the surface of iron oxide leading to the formation of Fe-oxalate complexes, and simultaneously the non-reductive/reductive dissolution of iron oxide takes place [9-13]. Light irradiation can greatly enhance the reductive dissolution of Fe(III)-oxalate complexes, yielding Fe(II) and oxalate radical $(C_2O_4)^{\bullet-}$ [6-13]. In the presence of O_2, the most reactive oxidant, •OH, can be obtained by the Fenton reaction of H_2O_2 with Fe(II), and iron cycling involving a series of active radicals can take place in the system [2-3, 13-15].

Compared with classical photo-Fenton systems (Fe^{2+} or Fe^{3+}/H_2O_2), the photo-Fe-oxalate system can form H_2O_2 in situ, and has the higher efficiency for the degradation of organic compounds [1, 14, 16]. While the homogeneous Fe-oxalate systems have been explored in many previous studies [1-3, 14-20],theheterogeneous Fe-oxalate systems, which do not easily bring about the secondary contamination of

abundant dissolved Fe ions in practical applications, have only received scant attention.

In the heterogeneous system, various iron (hydr)oxides demonstrate different dissolution properties [8]. The preparation method and intrinsic structure largely influence the activities of iron oxides [21-23]. Doping agents also significantly affect the photocatalytic activity of iron oxides [24, 25]. In the irradiated heterogeneous iron oxide-oxalate system, iron cycling, which happens both heterogeneously and homogeneously [6-8, 10], is essential because it produces H_2O_2 and •OH continuously. However, studies of the dissimilarities of iron oxides with different crystal structures in degrading contaminants and especially the generation of H_2O_2 and the different Fe species are scant, but are very important for understanding such complicated heterogeneous reactions.

In the present study, pentachlorophenol (PCP) was chosen as a probe pollutant because of its persistence in the environment and high toxicity due to the five chlorine atoms in its structure. The aim of this study was at comparing the activities of two iron oxides (goethite and hematite) in degrading PCP with oxalate under UV illumination,and investigating the formation of H_2O_2 and the adsorbed/dissolved Fe species cycling. In addition, the dechlorination, detoxification (Microtox acute toxicity) and intermediates of PCP were also investigated.

2. Experiments and Methods

2.1 Chemicals

PCP (98%) chemical was purchased from Aldrich, USA. Tetrachloro-*p*-benzoquinone (99%), tetrachloro-*o*-benzoquinone (97%), methanol (HPLC grade) and hexane (HPLC grade) chemicals were obtained from Acros, Belgium. Other chemicals with analytical gradewere purchased from Guangzhou Chemical Co. China. All the chemicals were used as received except acetic anhydride, which was redistilled for GC/MS analysis.

Deionized water (18.2 mΩ cm) from an ultrapure water system (Easy Pure'II RF/UV, USA) was used in all experiments. Goethite (α-FeOOH) and hematite (α-Fe_2O_3) powders were synthesized according to the procedures previously reported [26]. Whiletheir composition and crystal structures were confirmed by X-ray powder diffraction (XRD), their specific surface areas were measured to be 32.3 and 29.4 m^2 g^{-1}, respectively by the Brunauer–Emmett–Teller (BET) method..

2.2 Photochemical experiment

Aqueous PCP stock solution (0.075 mM) was prepared with 1.0% (v/v) ethanol and stored in a dark-brown glass bottle to avoid any photochemical reaction. In all photodegradation experiments, aqueous suspensions contained the same initial PCP concentration (0.0375 mM) and the same iron oxide content (0.4 g L^{-1}), but different initial concentrations of oxalic acid (C^0_{ox}). Ethanol was used to prepare the above aqueous PCP solutions andits concentration in all experiments was kept strictly at 0.5% as it is an •OH scavenger. It is believed that the ethanol would affect PCP degradation to a similar extent in all experiments, but should not affect the pattern of PCP degradation kinetics. All experiments were carried out in a photochemical reactor system described with details previously [10 at 30°C using a thermostatted water bath. Prior to UV light irradiation, adsorption/desorption equilibrium in the aqueous PCP suspension was established in the dark for 30 min. The suspension was continuously stirred by a magnetic stirrer andbubbled with air throughout each experiment. The water samples for HPLC, IC and GC-MS analyses were taken at various time intervals and then were centrifuged at 4500 rpm for 25 min, and further filtered through a 0.45 μm filter before injecting into the analytical instruments.. The initial pH of suspensions was adjusted to 3.5 using NaOH or $HClO_4$ solution.

105 **2.3 Analysis**

106 PCP and its reaction intermediates were determined by HPLC (Waters 1525/2487)
107 with an Xterra C18 reverse-phase column. For PCP analysis, a mobile phase containing
108 1% acetic acid in water/methanol (20:80 v/v) mixed solvent flew at arate of 1.0 mL min^{-1}.
109 The column temperature was set at 35 ^{o}C and UV detection was set at 295 nm. Following
110 the analytical procedure described by Oturan et al. [27], tetrachloro-*p*-benzoquinone and
111 tetrachloro-*o*-benzoquinone were identified by comparing their retention times with
112 internal standards. The mobile phase and flow rate were the same as the noted above, but
113 the ratio of 1% acetic acid in water to methanol was 25:75 (v/v), and the column
114 temperature and the detector wavelength were set at 30 ^{o}C and 280 nm, respectively.

115 The concentrations of oxalic acid and chloride ions were determined by ion
116 chromatography (IC Dionex ICS-90) with a mobile phase of aqueous 1.0 mM
117 $NaHCO_3$-8.0 mM Na_2CO_3 solution at a flow rate of 1.0 mL min^{-1}. An LC-10A system
118 (Shimadzu) with IC-A3 column was used to identify the intermediate products (HCOOH
119 and CH_3COOH) with a mobile phase of 2.5 mM phthalic acid and 2.4 mM Tris solution
120 at a flow rate of 1.2 mL min^{-1} and 40 ^{o}C.

121 H_2O_2 in aqueous solution was measured using an H_2O_2 analyzer (Lovibond-ET8600,
122 Germany), in which Lovibond reagent was reacted with H_2O_2 in a 10 mL vessel to form a
123 colored solution, and the concentration of H_2O_2 was determined photometrically at 528
124 nm with a detection limit of 0.05 mg L^{-1}. The Lovibond reagent was first added in the
125 vessel before the sample was taken from the photoreactor. At each time interval, 10 mL
126 of reaction solution was sampled and immediately filtered through a 0.45 μm filter before
127 it was placed into the vessel, and the concentration of H_2O_2 in the filtrate was measured
128 at once. Afterthis procedure was completed for one min, the validity of H_2O_2
129 concentration was ensured.

130 A GC-MS (Thermo Trace-DSQ-2000) system with electron ionization and an Agilent
131 silicon capillary column (0.25 mm × 30 m) was used to determine other products from

PCP degradation in which the samples were pretreated by extraction as the described previously [28, 29].

A Microtox analyzer (Strategic Diagnostics Inc., U.S. Model 500) was used to measure the Microtox acute toxicity of samples,in which the relative degree of sample toxicity is expressed by the percentage of light loss. The details of the measurement method can be found elsewhere [13].

Dissolved Fe(II) was measured colorimetrically by the ferrozine method and total dissolved iron was determined in the same way after adding 10% $OHNH_3Cl$ to reduce all Fe(III)(aq) to Fe(II)(aq). The adsorbed Fe(III)/Fe(II) on the surface of iron oxide was extracted by 0.1 M HCl solution with stirring for 30 min in the dark prior to the above analyses. Since no iron ion was detected in the α-FeOOH/α-Fe_2O_3 suspensions in the absence of oxalic acid under this extraction condition, it indicated that the fixed iron of α-FeOOH/α-Fe_2O_3 should not be extracted to interfere with the measurement of adsorbed Fe species. To avoid the oxidation of Fe(II), the sample filtered through the 0.45 μm filter was measured promptly after sample collection. In the measurement of Fe(III), several minutes were needed to allow complete reduction of Fe(III) to take place before addition of the buffer and ferrozine.

3. Results and Discussion

3.1 Photodegradation of PCP

The experimental results of PCP photodegradation under different conditions are presented in Figure 1. The results showed that 30-68% of PCP was removed after 1 h reaction time in the α-FeOOH suspension with different initial concentrations of oxalic acid (C^0_{ox}) (Figure 1A), which wasmuch lower than that (49-83%) in the α-Fe_2O_3 suspension (Figure 1B). In the absence of oxalic acid, PCP was only slightly degraded by direct photolysis at below 370 nm [28]. The results demonstrate that the presence of

158 oxalic acid greatly enhanced PCP degradation and an optimal C^0_{ox}inn the α-FeOOH and
159 α-Fe_2O_3 systemswas found to be around 1.2 mM. With this optimal C^0_{ox}, 68 and 83% of
160 PCP was photocatalytically degraded after 1 h in the α-FeOOH and α-Fe_2O_3 systems,
161 respectively.

162 The Fe species should play an important role in the PCP degradation because various
163 Fe species have different photoactivity [1, 9, 18]. For example, Fe(III) in the form of
164 $Fe(C_2O_4)_2^-$ and $Fe(C_2O_4)_3^{3-}$ can be more efficiently photolyzed to Fe(II) than as other
165 species [1, 9, 19], and Fe(II) as $Fe(C_2O_4)_2^{2-}$ can react with H_2O_2 to form •OH at a much
166 faster rate than that as Fe^{2+} [1, 9, 19]. According to the method described by Panias et al.
167 [4], the fractions of different Fe species in iron oxide-oxalate suspensions can be
168 calculated as the functions of pH and oxalic acid concentration. Using the tested pH
169 values and oxalic acid concentrations during the experiments, the changes in distribution
170 of different Fe(III)/Fe(II) species during the reaction time in the α-FeOOH or α-Fe_2O_3
171 suspension were calculated accordingly [13]. In the α-FeOOH or α-Fe_2O_3 suspension
172 during the photoreaction, the Fe(III) species $Fe(C_2O_4)_2^-$ and/or $Fe(C_2O_4)_3^{3-}$ with high
173 photoactivity were found to be the dominant species (> 90%) at different C^0_{ox}. For Fe(II)
174 species in the two suspensions, it was found that at C^0_{ox} = 0.4 mM, the Fe^{2+} species with
175 low photoactivity was the dominant species (> 60%). At 0.4 mM < C^0_{ox} < 1.2 mM, the
176 amounts of Fe^{2+} and $Fe(C_2O_4)_2^{2-}$ were similar with a total Fe(II) species fraction of >
177 90%, and at $C^0_{ox} \geq$ 1.2 mM, $Fe(C_2O_4)_2^{2-}$ became the dominant Fe(II) species (> 80%).
178 Consequently, it is reasonable to assume that at C^0_{ox} = 1.2 mM in the α-FeOOH or
179 α-Fe_2O_3 suspension, the two species of Fe (III) as $Fe(C_2O_4)_3^{3-}$ and Fe(II) as $Fe(C_2O_4)_2^{2-}$
180 with high photoactivity were formed to a sufficient extent to cause PCP degradation.
181 However, since oxalic acid itself was also a scavenger of •OH, , the reaction rate of PCP
182 degradation decreased at C^0_{ox} > 1.2 mM.

183 **[FIGURE 1]**

3.2 Dechlorination and detoxification of PCP

The ratio of dechlorination (%) was calculated as $[Cl^-]/[T\text{-}Cl_0]$ where $[Cl^-]$ is the concentration of chloride released from PCP degradation and $[T\text{-}Cl_0]$ is the stoichiometric concentration of organic chlorine in PCP. Figure 2 shows the rates of dechlorination in the two iron oxide systems with oxalate under UVA illumination. After 1 h reaction time,the dechlorination in the α-FeOOH system was achieved by 2-16% (Figure 2A), which was much lower than that in the $\alpha\text{-}Fe_2O_3$ system (7-28%) (Figure 2B). The amount of released chloride was much higher in the presence than in the absence of oxalic acid. The highest rate of dechlorination was obtained at the optimal C^0_{ox} of1.2 mM in both the α-FeOOH and $\alpha\text{-}Fe_2O_3$ suspensions. Furthermore, as the described previously [13,] the dechlorination reaction continued in the reactions with intermediate products after 1 h reaction time (data not shown here). Oturan *et al*. reported a similar phenomenon for PCP degradation in an electro-Fenton system [27]. These results may indicate that the cleavage of Cl-C bonds due to •OH attack has no preference compared to other degradation reactions in the system.

The data in Figure 3 confirmed the detoxification of PCP in terms of light loss determined with the Microtox analysis. At C^0_{ox} = 1.2 mM, the ratios of light loss after 1 h reaction decreased from 83 and 84% for the α-FeOOH and $\alpha\text{-}Fe_2O_3$ systems to 54 and 46%, Respectively. It is also proposed that the detoxification reaction continued with extension of the reaction time beyond 1 h as reported previously [13]. In addition, it is apparent that the results of dechlorination and detoxification were consistent in line with the PCP degradation, indicating that PCP was more efficiently degraded in the $\alpha\text{-}Fe_2O_3$ system than that in the α-FeOOH system.

[FIGURE 2]

[FIGURE 3]

3.3 Intermediates from PCP degradation

Although PCP was degraded in the α-FeOOH and α-Fe_2O_3 systems at different rates, the same intermediates were identified in the two systems with oxalic acid under UVA illumination, including tetrachlorocatechol (TeCC) and 2,3,5,6-tetrachloro-1,4-hydroquinone (TeCHQ) by GC-MS, tetrachloro-*o*-benzoquinone (*o*-chloranil) and tetrachloro-*p*-benzoquinone (*p*-chloranil) by HPLC, and HCOOH and CH_3COOH by IC.

Hydroquinone has been found to be a catalyst in the Fenton reaction to rapidly reduce Fe(III) to Fe(II)through an intermediate cycling by generation of a semiquinone product [30, 31], in which, hydroquinone reduces Fe(III) to form semiquinone and the semiquinone reduces Fe(III) to form quinone, while hydroquinone and quinone can be renewably formed by the dismutation of semiquinone [30, 31]. Such a intermediate cycling involving the reduction of Fe(III) can combine with the iron cycling of the system to accelerate the generation of Fe (II) and active species [31]. The intermediate cycling is described by equations (1)-(4), and the results in section 3.5 showed that more H_2O_2 was formed in the presence than in the absence of PCP, indicating the existence of the intermediate promotion mechanism involving the iron cycling.

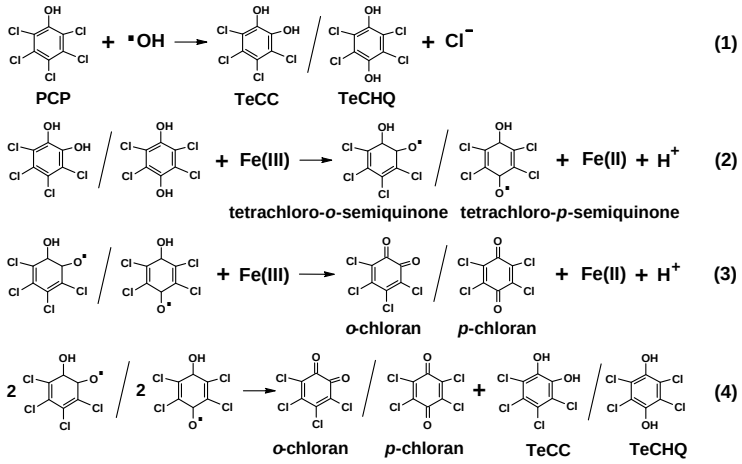

The above intermediate cycling can explain to some extent why production of $Cl_3C_6(OH)_3$ was not detected, because the oxidation to tetrachloro benzoquinone is more

favorable compared with further hydroxylation of the ring in such systems. Augusti *et al.* [32] reported similar results for chlorobenzene degradation by Fenton's reagent. The formation of organic acids with small molecule such as HCOOH and CH_3COOH confirmed that PCP was mineralized to some extent after its aromatic ring was brokenafter 1 h reaction time.

The control experiments showed that CH_3COOH was formed by oxidation of PCP and/or ethanol. Since the formation and degradation of intermediate products occurred at the same time, it was difficult to quantify the contribution of PCP to the fraction of CH_3COOH formation. Two other intermediates, tetrachloro-*p*-benzoquinone (*p*-chloranil) and HCOOH, were quantified as shown in Figure 4. It was found that the concentrations of the two intermediates in the α-FeOOH system were significantly higher than those in the α-Fe_2O_3 system. The results in sections 3.1 and 3.5 showed that the both rates of PCP degradation and H_2O_2 formation in the α-FeOOH suspension were significantly lower than those in the α-Fe_2O_3 suspension. All of these results indicated that more active substances could be generated in the α-Fe_2O_3 suspension to degrade the intermediates from PCP degradation. The shorter lifetime of these intermediates resulted in less accumulation in the α-Fe_2O_3 suspension.

[FIGURE 4]

3.4 Iron cycling during PCP degradation

Iron cycling is a key step in the Fenton reaction to continuously form H_2O_2 and •OH in an iron oxide-oxalate system, either in the dark or under light irradiation, as shown below [4-8]:

In the dark:

$$\equiv Fe^{III}(C_2O_4)_n^{3-2n} \leftrightarrow \equiv Fe^{II}(C_2O_4)_n^{2-2n} \quad [5] \qquad (5)$$

Under light irradiation:

$$\equiv Fe^{III}(C_2O_4)_n^{3-2n} \xrightarrow{h\nu} \equiv Fe^{II}(C_2O_4)_n^{2-2n} + (C_2O_4)^{\bullet-} \quad [1] \qquad (6)$$

$$Fe^{III}(C_2O_4)_n^{3-2n} + O_2^{\bullet-}/\bullet OOH / CO_2^{\bullet-} \xrightarrow{h\nu} Fe^{II}(C_2O_4)_n^{2-2n} + O_2 / (O_2 + H^+) / CO_2$$

k=10^4-10^9 M^{-1} s^{-1} [16, 33] (7)

$$Fe^{II}(C_2O_4)_n^{2-2n} + O_2^{\bullet-}/\bullet OOH + H^+ \xrightarrow{h\nu} Fe^{III}(C_2O_4)_n^{3-2n} + H_2O_2 \qquad k=10^5\text{-}10^7 \quad M^{-1} \quad s^{-1}$$

[33, 34] (8)

$$Fe^{II}(C_2O_4)_n^{2-2n} + H_2O_2 \rightarrow Fe^{III}(C_2O_4)_n^{3-2n} + \bullet OH + OH^- \quad k=3.1\times10^4\ M^{-1}\ s^{-1} \quad [16] \qquad (9)$$

In addition, the interface transfer process should be involved throughout the iron cycling:

$$2 \equiv Fe^{II}(C_2O_4)_n^{2-2n} \leftrightarrow 2Fe^{II}_{(aq)} + 2nCO_2 + nC_2O_4^{2-} \quad [33] \qquad (10)$$

$$\equiv Fe^{III}(C_2O_4)_n^{3-2n} \leftrightarrow (Fe^{III}(C_2O_4)_n^{3-2n})_{(aq)} \quad [33] \qquad (11)$$

The mechanism of iron cycling in the iron oxide-oxalate-UV system in the presence of PCP[delete?] is presented in Scheme 1. This cycling takes place simultaneously both on the surface of iron oxide and in the bulk solution. The hydroquinone/quinone intermediates of PCP can catalyze this cycling as the discussed above (Eqs. (1)-(4)). The interface transfer processes (Eqs. (10)-(11)) of Fe(III)/Fe(II) play an important role in the interaction between surface reaction and solution reaction.

To quantitatively study the iron cycling during PCP degradation, the concentrations of adsorbed and dissolved Fe(III)/Fe(II) versus reaction time were determined as shown in Figure 5. The concentration of adsorbed/dissolved Fe(III)/Fe(II) was mainly in the range 0.01-0.10 mM, which was much lower than the stoichiometric concentration corresponding to 0.4 g L^{-1} of α-FeOOH/α-Fe_2O_3 and the initial concentration of oxalic acid used. However, Zuo et al. [2-3] reported that H_2O_2 and •OH could be formed at much lower concentrations of Fe(III) (1 μM) and oxalate (5 μM), indicating that the amounts of Fe(III)/Fe(II) in our experiments were sufficient to form H_2O_2 and •OH.

After 30 min of adsorption/desorption equilibration in the dark, the concentration of adsorbed Fe(III) increased with the increase of C^0_{ox} in both the α-FeOOH and α-Fe_2O_3

systems. Only small amounts of dissolved Fe(III) and Fe(II) were formed by desorption of surface Fe(III)-oxalate complexes (Eq. (11)) and the slow reductive dissolution in the dark (Eq. (5)).

Figure 5 indicates that the amounts of all Fe species during photodegradation of PCP varied greatly in the initial stages of reaction, which might result from the fast redox cycling of Fe(III)/Fe(II) with vigorous interface transfer. It is known that light irradiation can greatly enhance the photochemical electron transfer of Fe(III)-oxalate complexes (Eq. (6)-(9)) [5-8]. In the late stage of reaction, the variation of the amounts of the different Fe species declined significantly, which might result from the loss of oxalic acid and the increase of pH. Correspondingly, as shown in Figure 1, the degradation of PCP in the α-FeOOH or α-Fe_2O_3 suspension had the same pattern of rapid degradation in the initial stage and gradually decreasing degradation rate in the later stage.

In the study [35], different iron oxides with almost the same concentration of total dissolved Fe showed different activities toward degradation of mordant yellow 10 (MY 10) in the iron oxide-H_2O_2 suspension. In this study, it was found that the concentrations of dissolved Fe(III)/Fe(II) in the α-FeOOH system were higher than in the α-Fe_2O_3 system during the reaction time as shown in Figure 5. However, PCP degradation in the α-FeOOH system was slower than in the α-Fe_2O_3 system. These results indicated that the amount of dissolved iron is not a rate-determining factor in relation to the activity of the iron oxides with different crystal structures. The exact mechanisms determining the activity of different iron oxides may involve their specific surface characters and the specific properties of target pollutants that need to be explored in further research.

In these heterogeneous iron oxide-oxalate systems, the dissolved Fe(II)/Fe(III) resulted from the redox reaction of Fe(III)/Fe(II) in solution, and also the interface transfer of Fe(II)/Fe(III) on the surface. As shown in Figure 5, it is interesting that the amounts of adsorbed Fe(II)/Fe(III) in the α-FeOOH or α-Fe_2O_3 system remained almost constant

during the late stage of reaction, indicating that the interface transfer process of Fe(II)/Fe(III) from surface to solution became slow due to the consumption of oxalic acid with pH increase, and might be a relatively slow process during the iron cycling. Sulzberger *et al.* and Banwart *et al.* noted that the interface process of detachment of Fe(II) from the surface was the rate-determining step in an iron oxide-oxalate-UV system [8-9, 36]. The results of this study should provide useful information to better understand the role of the interface transfer process during iron cycling in such heterogeneous systems.

[SCHEME 1]

[FIGURE 5]

3.5 Formation of hydrogen peroxide.

The most reactive oxidant, •OH, is obtained through the H_2O_2 reaction with Fe(II), while H_2O_2 is mainly generated by the reaction of Fe(II) with $O_2^{\bullet-}$/•OOH and the dismutation of $O_2^{\bullet-}$/•OOH in the presence of O_2 [1-3]. The concentration of H_2O_2 in the system depends on both the rates of its generation and consumption. The more rapid is iron cycling, the greater amount of H_2O_2 can be formed. The variation of H_2O_2 concentration vs. reaction time in the α-FeOOH and α-Fe_2O_3 suspensions is presented in Figure 6.

In the absence of oxalic acid, H_2O_2 was not detected during 60 min in the α-FeOOH or α-Fe_2O_3 system. In the presence of oxalic acid, H_2O_2 was detected at a significant level between 0.1-1.2 mg L^{-1} in the α-FeOOH suspension (Figure 6A) and 1.2-3.0 mg L^{-1} in the α-Fe_2O_3 suspension (Figure 6B). In both the α-FeOOH and α-Fe_2O_3 systems, more H_2O_2 could be formed in the presence than in the absence of PCP at C^0_{ox} = 1.2 mM, and the concentrations of H_2O_2 at $C^0_{ox} \geq 1.2$ mM were much higher than at C^0_{ox} = 0.4 mM. It was apparent that the concentration of H_2O_2 in the α-Fe_2O_3 system was significantly

higher than that in the α-FeOOH system.

The above results may explain why PCP was more effectively photodegraded in the α-Fe_2O_3 system. In addition, the above results to a certain extent confirmed that the hydroquinone intermediates could accelerate iron cycling and promote the formation of active compounds as discussed in sections 3.3 and 3.4.

The Fe(III)-oxalate complexes are initially formed by the adsorption of oxalic acid [9, 13]. Then the photo-reduction of Fe(III)-oxalate complexes can generate H_2O_2 and a series of active radicals [1-3]. Thus, the amount of oxalic acid adsorption on the surface of iron oxide directly influenced the formation of H_2O_2. However, the adsorption abilities of different iron oxides are different due to different surface properties and crystal structures.

Recently, we systematically studied the adsorption behavior of oxalic acid on the surface of different iron oxides, including some important and effect factors. It was found that the ability of α-Fe_2O_3 to adsorb oxalic acid was much stronger than that of α-FeOOH, and the adsorption of oxalic acid approached its maximum amount at about C^0_{ox} = 1.2 mM on both iron oxides, which is consistent with the results of H_2O_2 formation in the present study. The detailed results of these adsorption experiments will be reported in another paper.

[FIGURE 6]

4. Conclusions

68 and 83% of PCP were photodegraded after 1 h reaction at C^0_{ox} = 1.2 mM in aqueous goethite and hematite suspensions, respectively. Dechlorination and detoxification (Microtox acute toxicity) of PCP were also achieved to a greater extent in the hematite suspension than in the goethite suspension, indicating that hematite has the higher activity than goethite for PCP degradation in such an iron oxide-oxalate system under

360 UVA illumination. The experiments further confirmed that more H_2O_2 could be formed in
361 the hematite system than in the goethite system due to the more rapid iron cycling, which
362 is beneficial to enhance the PCP degradation.
363
364 **Acknowledgment**
365 The authors appreciate the financial support by the National Science Foundation of China
366 (No. 40771105).
367
368 **Literature Cited**
369 [1] M.E. Balmer, B. Sulzberger, Atrazine degradation in irradiated iron/Oxalate systems:
370 effects of pH and oxalate. Environ. Sci. Technol. 33 (1999) 2418-2424.
371 [2] Y.G. Zuo, J. Hoigne, Evidence for photochemical formation of H_2O_2 and oxidation of
372 SO_2 in authentic fog water. Science. 260 (1993) 71-73.
373 [3] Y.G. Zuo, J. Hoigne, Formation of hydrogen peroxide and depletion of oxalic acid in
374 atmospheric water by photolysis of iron(III)-oxalato complexes. Environ. Sci.
375 Technol. 26 (1992) 1014-1022.
376 [4] D.Panias, M. Taxiarchou, I. Douni, I. Paspaliaris, A. Kontopoulos, Thermodynamic
377 analysis of the reactions of iron oxides: dissolution in oxalic acid. Can. Metal. Quart.
378 35 (1996) 363-373.
379 [5] D. Panias, M. Taxiarchou, I. Paspaliaris, A. Kontopoulos, Mechanisms of dissolution
380 of iron oxides in aqueous oxalic acid solutions. Hydrometallurgy. 42 (1996) 257-265.
381 [6] M.I. Litter, E.C. Baumgartner, G.A. Urrutla, M.A. Blesa, Photodissolution of iron
382 oxides. 3. Interplay of photochemical and thermal processes in maghemite/carboxylic
383 acid systems. Environ. Sci. Technol. 25 (1991) 1907-1913.
384 [7] C. Siffert, B. Sulzberger, Light-Induced dissolution of hematite in the presence of
385 oxalate: a case study. Langmuir. 7 (1991) 1627-1634.

386 [8] B. Sulzberger, H. Laubscher, Reactivity of various types of iron(III) (hydr)oxides
387 towards light-induced dissolution. Marine Chem. 50 (1995) 103-115.
388 [9] P. Mazellier, B. Sulzberger, Diuron degradation in irradiated, heterogeneous
389 iron/oxalate systems: The rate-determining step. Environ. Sci. Technol. 35 (2001)
390 3314-3320.
391 [10] F.B. Li, X.Z. Li, X.M. Li, T.X. Liu, J. Dong, Heterogeneous photodegradation of
392 bisphenol A with iron oxides and oxalate in aqueous solution. J. Colloid Interf. Sci.
393 311 (2007) 481-490.
394 [11] C.S. Liu, F.B. Li, X.M. Li, G. Zhang, Y.Q. Kuang, The effect of iron oxides and
395 oxalate on the photodegradation of 2-mercaptobenzothiazole. J. Mol. Catal.
396 A-Chem. 252 (2006) 40-48.
397 [12] X.G. Wang, C.S. Liu, X.M. Li, F.B Li, S.G. Zhou, Photodegradation of
398 2-mercaptobenzothiazole in the γ-Fe_2O_3/oxalate suspension under UVA light
399 irradiation. J. Hazard. Mater. 153 (2008) 426-433.
400 [13] Q. Lan, F.B. Li, C.S. Liu, X.Z. Li, Heterogeneous Photodegradation of
401 Pentachlorophenol with Maghemite and Oxalate under UVA Illumination. Environ.
402 Sci. Technol. 42 (2008) 7918-7923.
403 [14] D.L. Sedlak, J. Hoigné, The role of copper and oxalate in the redox cycling of iron
404 in atmospheric waters. Atmos. Environ. 27A (1993) 2173-2185.
405 [15] H. Liu, C. Wang, X. Li, X. Xuan, C. Jiang, H. Hui, A Novel electro-Fenton process
406 for water treatment: reaction-controlled pH adjustment and performance assessment.
407 Environ. Sci. Technol. *41 (*2007) 2937-2942.
408 [16] A. Safazadeh-Amiri, J.R. Bolton, S.R. Cater, Ferrioxalate-mediated
409 photodegradation of organic pollutants in contaminated water. Water Res. 31 (1997)
410 787-798.
411 [17] Y.G. Zuo, J. Zhan, Effects of oxalate on Fe-catalyzed photooxidation of dissolved

412 sulfur dioxide in atmospheric water. Atmos. Environ. *39 (*2005) 27-37.
413 [18] B.C. Faust, R.G. Zepp, Photochemistry of aqueous iron(III)-polycarboxylate
414 complexes: roles in the chemistry of atmospheric and surface waters. Environ. Sci.
415 Technol. 27 (1993) 2517-2522.
416 [19] J.S. Jeong, J.Y. Yoon, pH effect on OH radical production in photo/ferrioxalate
417 system. Water Res. 39 (2005) 2893-2900.
418 [20] F. Wu, N. Deng, Y. Zuo, Discoloration of dye solutions induced by solar photolysis
419 of ferrioxalate in aqueous solutions. Chemosphere. 39 (1999) 2079-2085.
420 [21] X. Wang, L. Zhang, Y. Ni, J. H, X. Cao, Fast Preparation, characterization, and
421 property study of α-Fe_2O_3 nanoparticles via a simple solution-combusting method.
422 J. Phys. Chem. C. 113 (2009) 7003-7008.
423 [22] J. Yu, X. Yu, B. Huang, X. Zhang, Y. Dai, Hydrothermal synthesis and visible-light
424 photocatalytic activity of novel cage-like ferric oxide hollow spheres. Cryst.
425 Growth Des. 9 (2009) 1474-1480.
426 [23] J. Yu, G. Wang, B. Cheng, M. Zhou, Effects of hydrothermal temperature and time
427 on the photocatalytic activity and microstructures of bimodal mesoporous TiO_2
428 powders. Appl. Catal. B: Environ. 69 (2007) 171-180.
429 [24] M. Zhou, J. Yu, B. Cheng, Effects of Fe-doping on the photocatalytic activity of
430 mesoporous TiO_2 powders prepared by an ultrasonic method. J. Hazard. Mater. 137
431 (2006) 1838-1847.
432 [25] F.B. Li, X.Z. Li, C.S. Liu, T.X. Liu, Effect of alumina on photocatalytic activity of
433 iron oxides for bisphenol A degradation. J. Hazard. Mater. 149 (2007) 199-207.
434 [26] F.B. Li, X.G. Wang, Y.T. Li, C.S. Liu, F. Zeng, L.J. Zhang, M.D. Hao, H.D. Ruan,
435 Enhancement of the reductive transformation of pentachlorophenol by
436 polycarboxylic acids at the iron oxide-water interface. J. Colloid Interf. Sci. 321
437 (2008) 332-341.

438 [27] M.A. Oturan, N. Oturan, C. Lahitte, S. Trevin, Production of hydroxyl radicals by
439 electrochemically assisted Fenton's reagent: Application to the mineralization of an
440 organic micropollutant, pentachlorophenol. J. Electroanal. Chem. 507 (2001)
441 96-102.
442 [28] M. Fukushima, K. Tatsumi, K. Morimoto, Influence of iron(III) and humic acid on
443 the photodegradation of pentachlorophenol. Environ. Toxicol. Chem. 19 (2000)
444 1711-1716.
445 [29] M. Fukushima, K. Tatsumi, Degradation pathways of pentachlorophenol by
446 photo-Fenton pystems in the presence of Iron(III), humic Acid, and hydrogen
447 peroxide. Environ. Sci. Technol. 35 (2001) 1771-1778.
448 [30] R.Z. Chen, J.J. Pignatello, Role of Quinone Intermediates as Electron Shuttles in
449 Fenton and Photoassisted Fenton Oxidations of Aromatic Compounds. Environ. Sci.
450 Technol. 31 (1997) 2399-2406.
451 [31] F. Chen, W.H. Ma, J.J. He, J.C. Zhao, Fenton degradation of malachite green
452 catalyzed by aromatic additives. J. Phys. Chem. A. 106 (2002) 9485-9490.
453 [32] R. Augusti, A.O. Dias, L.L. Rocha, R.M. Lago, Kinetics and mechanism of benzene
454 derivative degradation with Fenton's reagent in aqueous medium studied by MIMS.
455 J. Phys. Chem. A. 102 (1998) 10723-10727.
456 [33] R.W. Matthews, The reaction chemistry of aqueous ferrous sulfate solutions at
457 natural pH. Aust. J. Chem. 36 (1983) 1305-1317.
458 [34] T.E. Graedel, M.L. Mandich, Kinetic model studies of atmospheric droplet
459 chemistry 2. Homogeneous transition metal chemistry in raindrops. Geophys. Res.
460 91 (1986) 5205-5221.
461 [35] J. He, W.H. Ma, J.J. He, J.C. Zhao, J.C. Yu, Photooxidation of azo dye in aqueous
462 dispersions of H_2O_2/α-FeOOH. Appl. Catal. B: Environ. 39 (2002) 211-220.
463 [36] S. Banwart, S. Davies, W. Stumm, The role of oxalate in accelerating the reductive

464 dissolution of hematite (α-Fe_2O_3) by ascorbate. Colloid and Surface. 39 (1989)
465 303-309.
466

Figure Captions

FIGURE 1. The photodegradation of PCP versus reaction time in irradiated heterogeneous systems with 0.4 g L^{-1} iron oxides and different C^0_{ox} at initial pH 3.5: (A) α-FeOOH suspension; (B) α-Fe_2O_3 suspension. The inserted plot shows the dependence of the first-order rate constant (*k*) of PCP degradation on C^0_{ox}.

FIGURE 2. The changes of dechlorination during PCP photodegradation in irradiated heterogeneous system with 0.4 g L^{-1} iron oxides and different C^0_{ox} at initial pH 3.5: (A) α-FeOOH suspension; (B) α-Fe_2O_3 suspension.

FIGURE 3. Detoxification of PCP during the reaction time at the optimal C^0_{ox} (1.2 mM) in α-FeOOH and α-Fe_2O_3 systems under UVA illumination.

FIGURE 4. Concentration changes of PCP intermediates versus reaction time at the optimal C^0_{ox} (1.2 mM) in α-FeOOH and α-Fe_2O_3 systems under UVA illumination. (A) p-chloranil; (B) HCOOH.

SCHEME 1. The mechanism of iron cycling with iron oxides and oxalate under UVA illumination in the presence of PCP. HQ and Q represent the hydroquinone (TeCC/TeCHQ) and quinone (*o*-chloranil/*p*-chloranil) intermediates detected. SQ represents the tetrachloro-*o*-semiquinone/tetrachloro-*p*-semiquinone radicals.

FIGURE 5. The concentration variation of adsorbed/dissolved Fe during PCP photodegradation for different C^0_{ox} in α-FeOOH and α-Fe_2O_3 systems. (A) the adsorbed Fe(III); (B) the adsorbed Fe(II); (C) the dissolved Fe(III); (D) the dissolved Fe(II).

493

494 **FIGURE 6.** The formation of H_2O_2 during PCP degradation in irradiated heterogeneous
495 system with 0.4 g L^{-1} iron oxides and different C^0_{ox} at initial pH 3.5. (A) α-FeOOH
496 system; (B) α-Fe_2O_3 system.

497

498 **FIGURE 1**

499

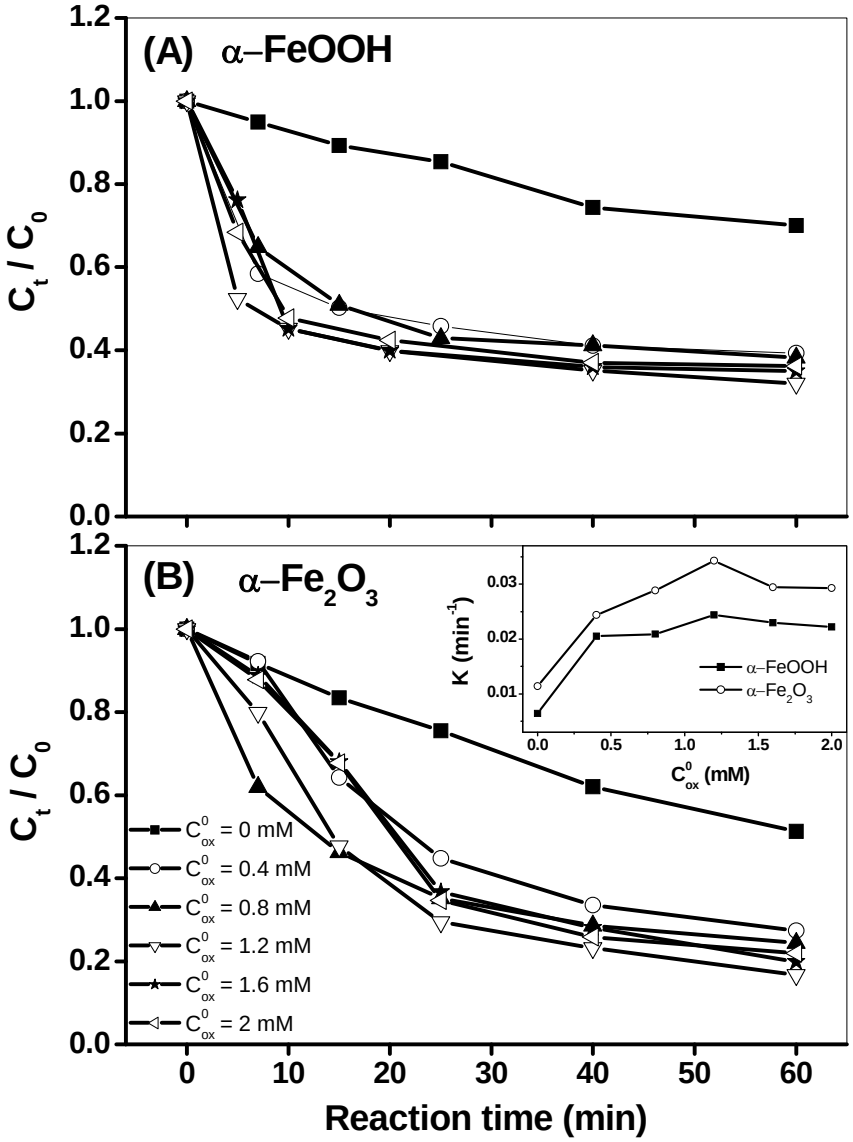

500

501

502 **FIGURE 2**

503

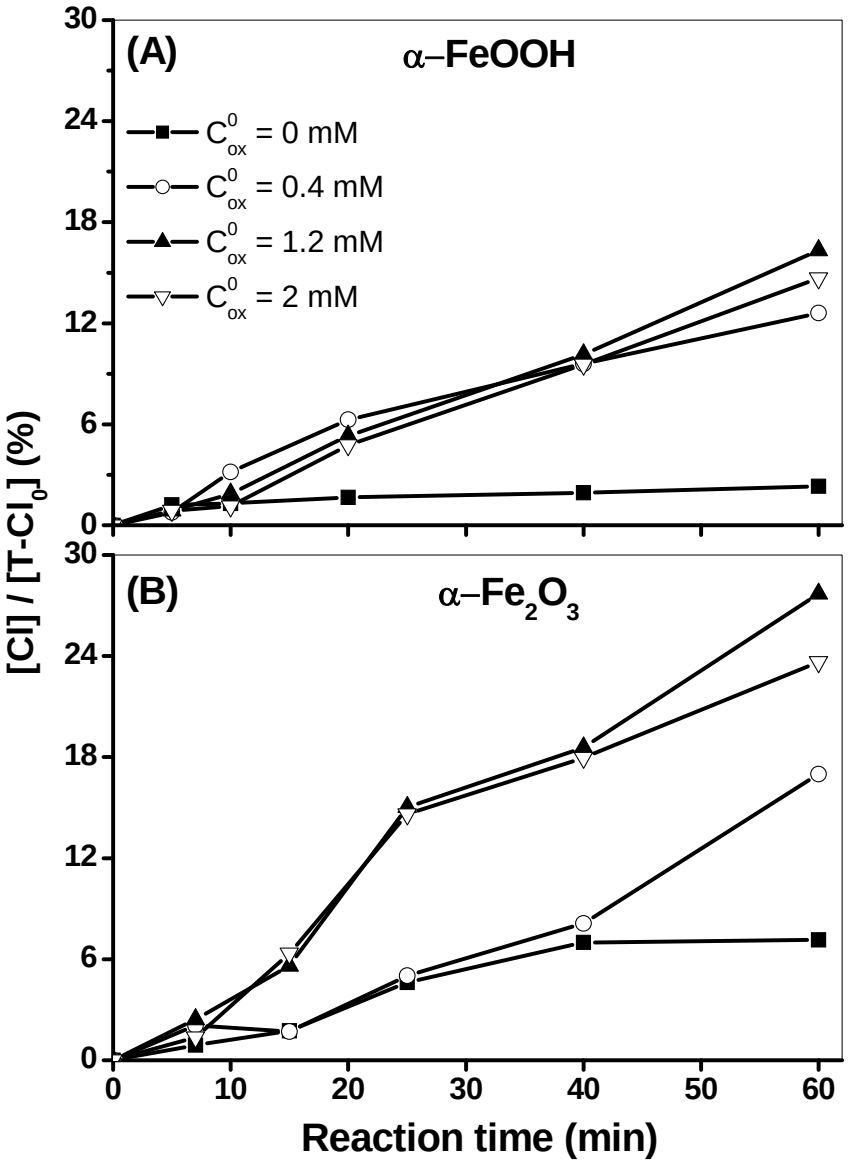

504

505

506 **FIGURE 3**

507

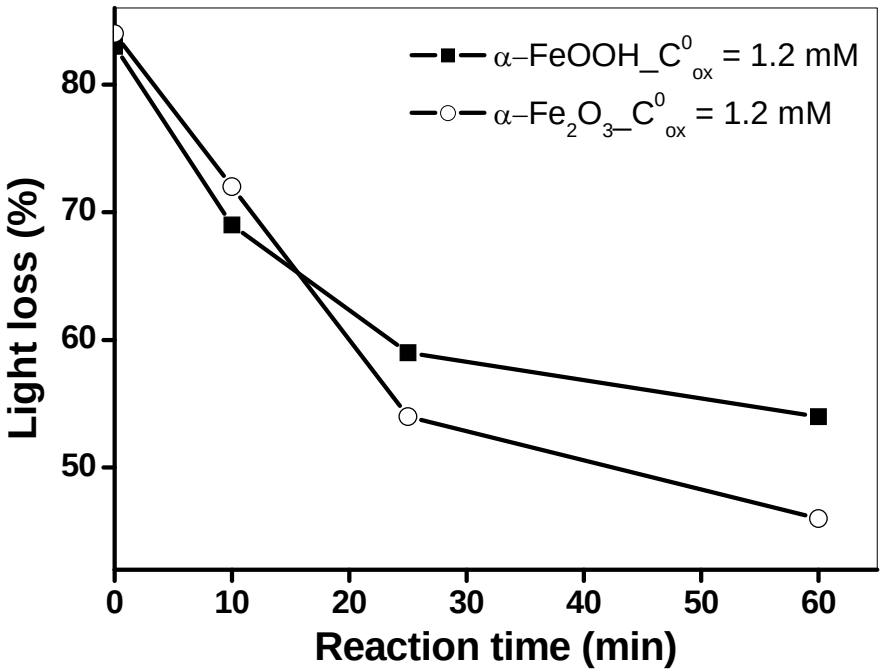

508

509

510 **FIGURE 4**

511

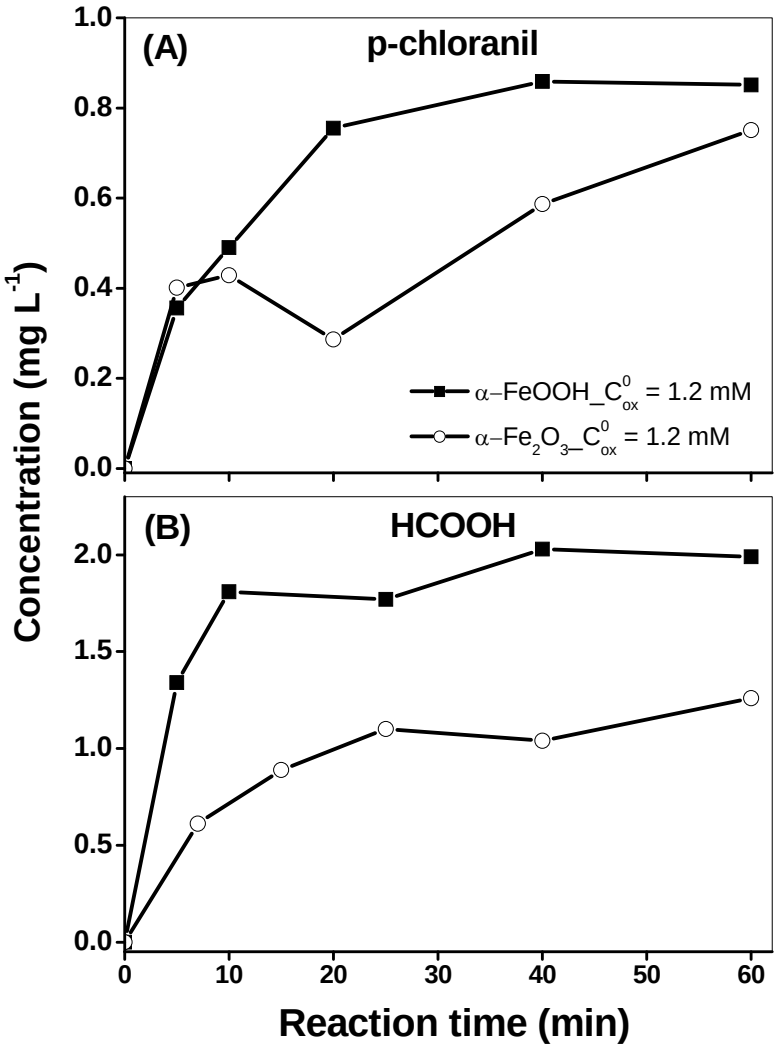

512

513 **SCHEME 1**

514

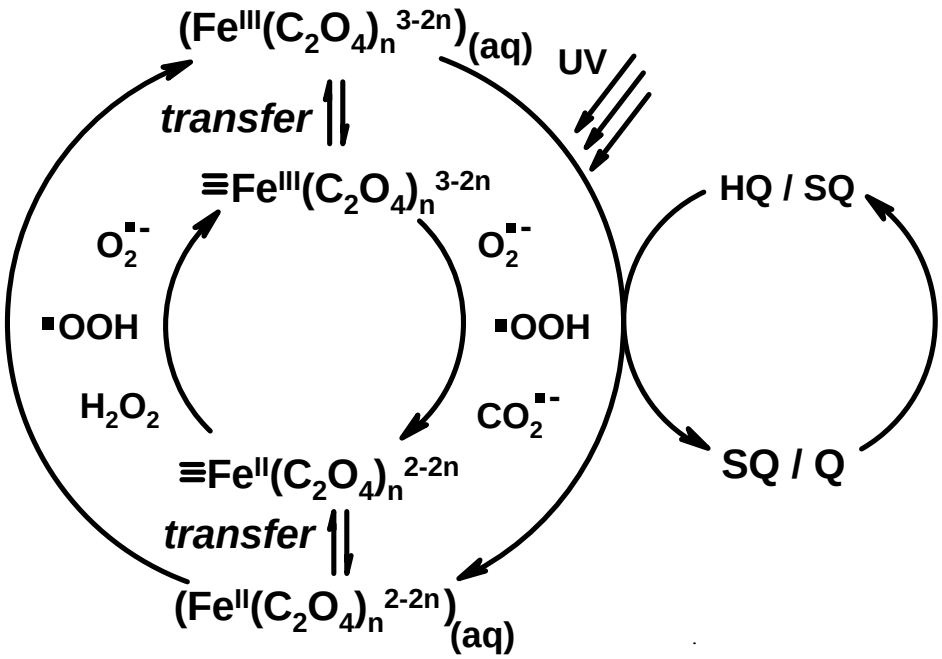

515

516

517 **FIGURE 5**

518

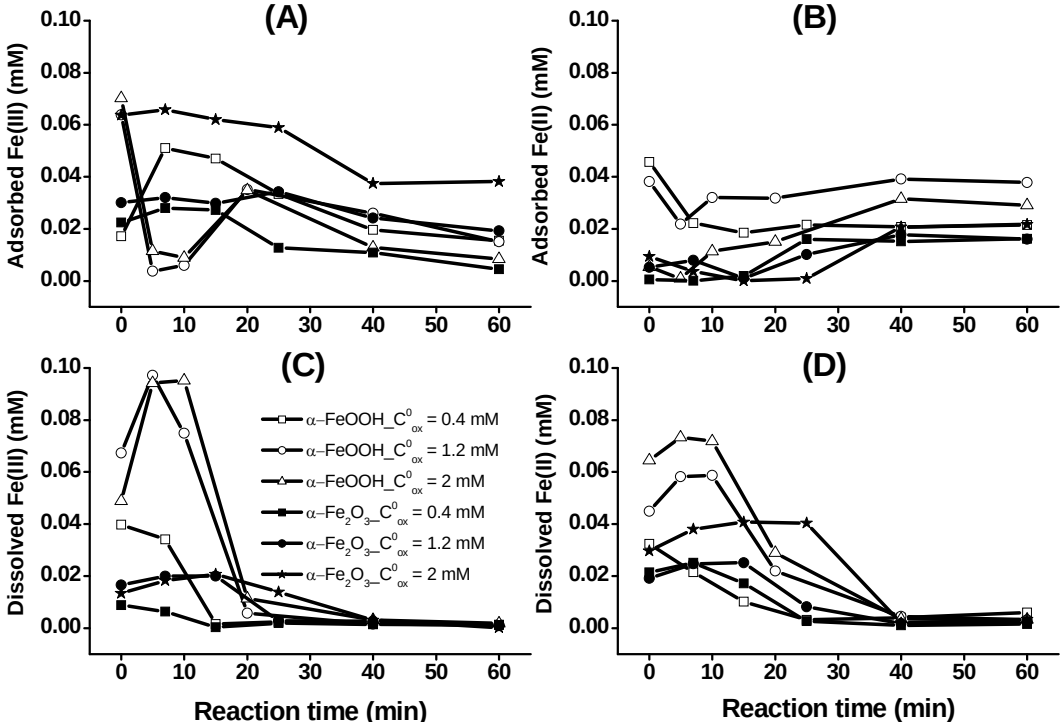

519

520

521 **FIGURE 6**

522

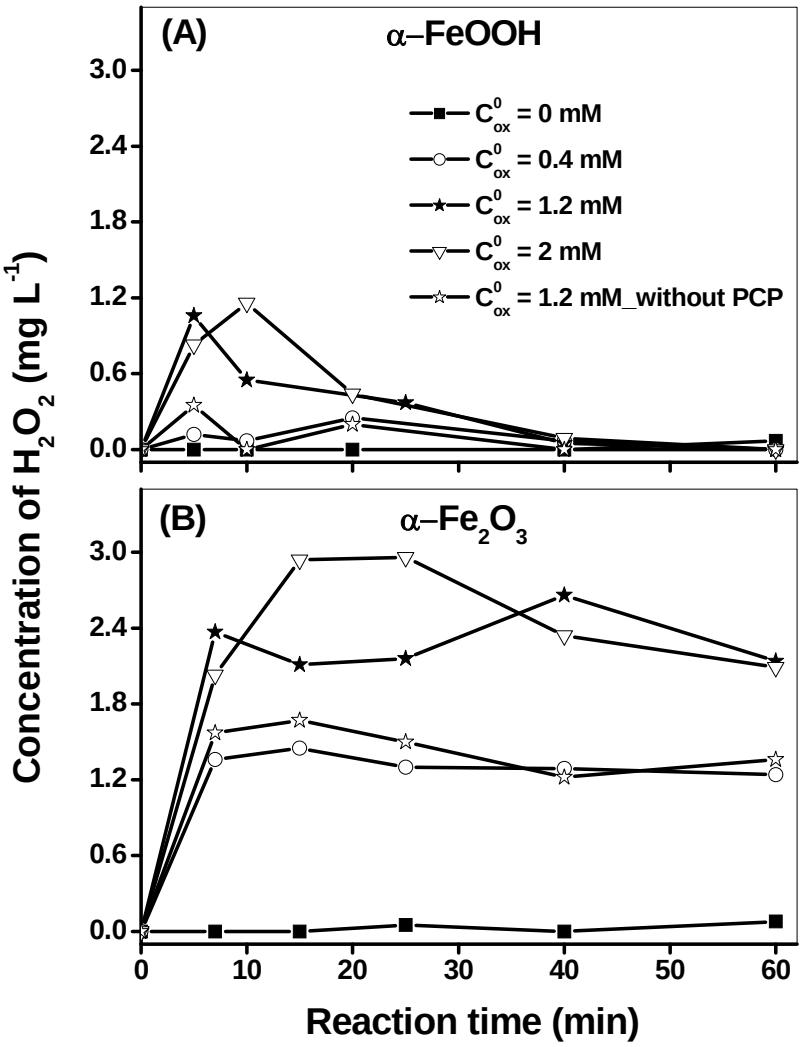

523